

# **THE ROLE OF NIOBIUM FOR THE DEVELOPMENT OF WEAR RESISTANT STEELS WITH SUPERIOR TOUGHNESS**

A.S. Schneider, J.L. Cayla, C. Just and V. Schwinn

AG der Dillinger Hüttenwerke, Research, Development and Plate-Design,  
P.O. Box 1580, 66748 Dillingen/Saar, Germany

Keywords: Niobium, Direct Quenching, Wear Resistant Steel, Recrystallization, Strength, Plate, Charpy Toughness, Finish Rolling Temperature, Hardness, EBSD, Microstructure, Grain Size

## **Abstract**

Wear resistant steels are commonly designed to have a high hardness and at the same time good weldability due to a low alloy content. The high hardness is achieved by quenching the material to a martensitic microstructure, which requires systematic alloying with Mn, Cr, Ni and Mo. However, even for wear resistant steels, a high toughness may be advantageous, as it not only ensures good impact resistance, even at sub-zero temperatures, but can enhance the wear resistance by causing a change in the wear mechanism. Besides a high level of process-based steel cleanliness, microalloying with Nb provides the basis to enhance the toughness of the steel. The objective of this paper is to present a selected study of how microalloying with Nb in combination with a well-adapted process route can be used to obtain wear resistant steels with a superior balance of toughness and hardness.

## **Introduction**

Based on their high hardness and low-to-medium C content, wear resistant steels exhibit an optimum combination of wear performance and workability. Typically, wear resistant steels are available with hardness levels varying from 300 to 600 HB and are used in the form of heavy plates or hot rolled strip. The high hardness in these steels is realized by a quenching treatment leading to a fully martensitic microstructure. To obtain a uniform martensitic structure or hardness across the entire plate thickness, within achievable quenching rates, the steel has to be alloyed with carbon and other elements, such as Mn, Cr, Ni and Mo. The quenching treatment can be either carried out off-line, via the conventional reheating and quenching (RQ) route or achieved by direct quenching (DQ) after hot rolling using in-line water cooling units.

The DQ process has several advantages over the RQ process. For example, the production costs and time can be significantly reduced by eliminating the additional reheating and cooling step. Furthermore, direct quenching immediately after the hot rolling allows for some control of the austenite structure prior to transformation. It is well known that the deformation of austenite refines the post-transformation products causing an increase of strength and toughness [1-5]. In addition, due to the higher austenitization temperature relative to the RQ process, even microalloying elements such as Nb can be dissolved in the DQ process, which results in a higher hardenability [4]. Accordingly, the desired mechanical properties can be achieved with a leaner chemistry and the content of costly alloying elements can be reduced in steels produced via

direct quenching. Additionally, the reduction of the alloying elements is beneficial for the weldability and the formability of the steel.

The structure of the austenite in the DQ process and thus the mechanical properties strongly depend on the specific hot rolling parameters. The most critical parameter in this respect is the finish rolling temperature (FRT). If the finish rolling temperature is significantly above the non-recrystallization temperature ( $T_{nr}$ ), a fully recrystallized austenite structure is obtained. This process is also referred to as hot rolling (HR). In contrast, if the rolling is performed at a lower temperature, only slightly above  $T_{nr}$ , grain growth is limited. Therefore, this process, referred to as recrystallized-controlled rolling (RCR), results in an austenite structure with fine and equiaxed grains. Nevertheless, because rolling is completed close to  $T_{nr}$ , a deformation substructure could be present in the steel. In the case of controlled rolling (CR), the FRT is lower than  $T_{nr}$ . As a consequence, the austenite grains are work hardened and elongated in the rolling direction. In the literature this structure is termed as a pancake microstructure.

Previous studies have shown that CR-DQ leads to a superior balance of strength and toughness compared to HR-DQ and RQ [3,5]. However, this is only true for steels with relatively large amounts of alloying elements, in which martensite formation occurs upon cooling despite the fine and heavily deformed austenite structure. The high strength in these steels is attributed to the refined post-transformation microstructure and the inheritance of the austenite deformation substructure in the martensitic phase, ie. the ausforming effect [4]. The improvement of toughness can also be explained by the refinement of the martensitic structure [4]. Furthermore, it has been suggested that the superior toughness is related to a crystallographic texture developed in the austenite prior to quenching, which can lead to delaminations or splitting in the Charpy specimens [2,3]. This has the beneficial effect of reducing the triaxial stress state at the crack tip and accordingly shifts the Charpy impact toughness transition temperature to lower values [6].

So far, only a few studies have investigated the effect of the CR-DQ process on the properties of wear resistant steels. To avoid the low ductility problems associated with fully martensitic microstructures in wear resistant steels with overall hardness levels above 500 HB, Kinnunen et al. performed rolling experiments using direct quenching from different final rolling temperatures [7]. The purpose of this study was to increase the toughness of the martensitic structure by incorporating a small amount of soft ferrite. However, their results indicated that the steel containing martensite and ferrite had a poorer abrasion resistance than the fully martensitic reference steel, which was attributed to the decrease in hardness with increasing ferrite content. Song et al. studied the microstructure and mechanical properties of a wear resistant steel with a C content of 0.17 wt.% produced via DQ and conventional RQ [8,9]. For a quenching temperature of 950 °C, in both processes, they observed superior mechanical properties for the DQ process compared to the RQ process. However, the hardly elongated grains visible in their optical micrographs indicate that rolling was completed at a temperature only marginally below  $T_{nr}$ .

Although these studies demonstrate the potential of the CR-DQ process, in both cases the rolling parameters were not chosen to optimize strength and toughness. In addition, as in most other studies on direct quenching, rolling and quenching were performed on a laboratory scale using plates with a length of not more than 1-2 m. Therefore, we investigated the influence of CR-DQ on the mechanical properties of wear resistant steel plates produced on a full-scale plate mill with lengths of several tens of meters. The uniformity of properties was assessed by testing the head and tail positions of each plate. To increase strength and toughness, FRTs significantly below  $T_{nr}$  were evaluated.

## Experimental

In this study, three continuously cast slabs with an initial thickness of 290 mm were rolled to a final thickness of 20 mm and direct quenched to room temperature using a Mulpic cooling device. Depending on the exact dimensions of the slabs, these plates had lengths varying from 22-28 m in the rolled condition.

The chemical composition of the steel is given in Table I. The basic heat contains approximately 0.15 wt.%C, 0.3 wt.%Si, 1.3 wt.%Mn and a small amount of Mo. In addition, the steel was microalloyed with Nb for austenite grain size control during processing. Nb is also crucial for the CR-DQ process, as it increases the  $T_{nr}$  and thus enables rolling in a temperature interval between  $Ar_3$  and  $T_{nr}$ .

Table I. Chemical Composition of the Investigated Steel

Element	C	Si	Mn	Additional alloys
wt. %	<0.15	0.3	1.3	Mo, Nb

Before rolling, the slabs were reheated at 1200 °C for several hours in a pusher furnace. The rolling included roughing passes at a high temperature to a constant intermediate thickness, a hold time in air and a final series of passes in a predefined temperature range close to the designated FRT. During hot rolling, the condition of the austenite was varied by applying three different FRTs with respect to the  $T_{nr}$ . The  $T_{nr}$  of the steel was calculated to be approximately 950 °C according to the equation developed by Boratto et al. [10]. To realize a fully recrystallized austenite structure before quenching, one plate was finish rolled at a temperature above the theoretical  $T_{nr}$ . This procedure will hereafter be referred to as hot rolling. In addition, two plates were controlled rolled at temperatures below  $T_{nr}$ . While for one of these plates rolling was completed only a few degrees below  $T_{nr}$  ( $FRT < T_{nr}$ ), for the other plate the FRT was significantly below  $T_{nr}$  ( $FRT \ll T_{nr}$ ).

The structure of the samples was examined by light optical microscopy and electron backscattered diffraction (EBSD). The metallographic samples were taken from both ends (head and tail) of each plate with the investigated cross-section parallel to the rolling direction. All samples were mechanically ground and polished by a conventional metallographic procedure. For the microstructural characterization in the optical microscope, the polished samples were etched in a 5% nital solution, while specimens for EBSD were electropolished using a Struers

electrolyte. The EBSD patterns were collected in a scanning electron microscope (Zeiss Supra VP 55) at an acceleration voltage of 25 kV and a working distance of 15 mm. The parent austenite grain structure was automatically reconstructed from the EBSD data by applying the ARPGE software [11]. This software uses an algorithm based on the general crystallographic relationship between martensite/bainite to determine which orientations are directly inherited from a unique parent grain (austenite).

Mechanical tests included measurements of hardness, tensile properties and impact toughness. As for the microstructural characterization, these tests were performed on samples taken from the head and the tail positions of each plate. For the tensile tests, full thickness flat tensile specimens were used and tested in accordance with the ISO 6892-1 specification. Charpy impact tests were conducted using standard V-notch samples as per the ISO 148-1 specification. The Charpy specimens with a cross-section of 10 x 10 mm were machined 2 mm beneath the surface in both the longitudinal and transverse directions of the 20 mm thick plates. The Charpy V-notch impact energy was determined at the following temperatures: -100 °C, -80 °C, -60 °C, -40 °C, -20 °C and 0 °C.

To assess the hardenability of the alloy for the applied rolling conditions, Vickers hardness profiles were determined across the thickness of the plates. The indents were performed with a maximum load of 100 N and a step size of 2 mm.

## Results

Figure 1 shows representative engineering stress-strain curves of samples taken from both ends of the plates finish rolled at different temperatures with respect to  $T_{nr}$ . In all cases, the plates exhibit a similar stress-strain behavior at the head and the tail positions as well as a continuous transition from elastic to plastic deformation. Depending on FRT, the ultimate tensile strength of the plates is in the range of 1200-1350 MPa and the strain to failure varies between 7.7% and 8.9%. The highest ultimate tensile strength, but also a slightly smaller strain to failure than for the other two plates is observed for the plate finish rolled at the lowest temperature. Despite different FRTs, the other two plates, finish rolled at the intermediate and at the highest temperature, demonstrate similar ultimate strength and strain to failure values.

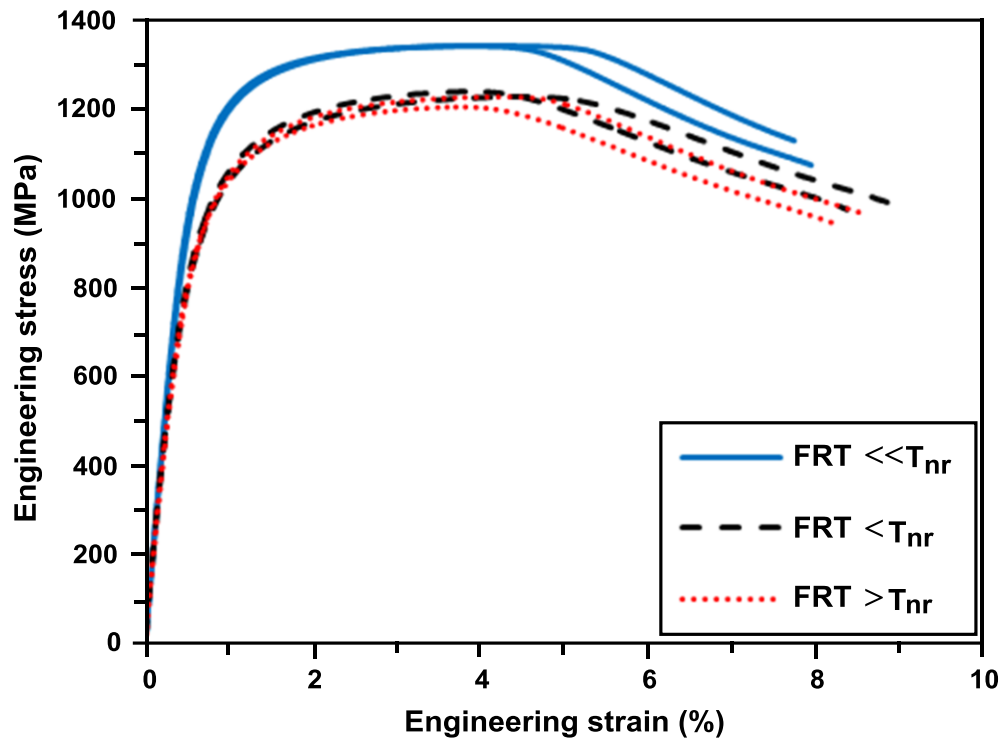


Figure 1. Representative engineering stress-strain curves of samples taken from the head and the tail positions of the plates finish rolled at different temperatures with respect to  $T_{nr}$ . For each plate, one curve is shown for the head and one for the tail position.

Charpy V-notch transition curves for samples oriented in the longitudinal and the transverse direction of the three plates are shown in Figure 2. Each data point in the plot represents the mean value of six individual Charpy V-notch tests performed on three samples from the head and three from the tail position of each plate. The small standard deviation represented by the error bars indicates that the measured impact energy is not significantly affected by the sample position, ie. is almost the same at both ends of the plates. However, it can be seen that the impact energy strongly depends on FRT and sample direction. For samples oriented in the transverse and the longitudinal direction, the impact energy increases with decreasing FRT. This is true for the entire range of test temperatures except at a test temperature of 0 °C, for which the plates finish rolled at temperatures close to  $T_{nr}$  exhibit virtually the same impact energy.

A comparison between Figures 2(a) and (b) further indicates that the longitudinal sample direction leads to higher impact energies than the transverse direction. However, this effect is only pronounced for the plate with the lowest FRT. For example, at a test temperature of 0 °C, the impact energy of this plate measured in the longitudinal directions is a factor of two larger than that measured in the transverse direction. In contrast, for the other two plates, the impact energy for both directions differs by only a few Joules.

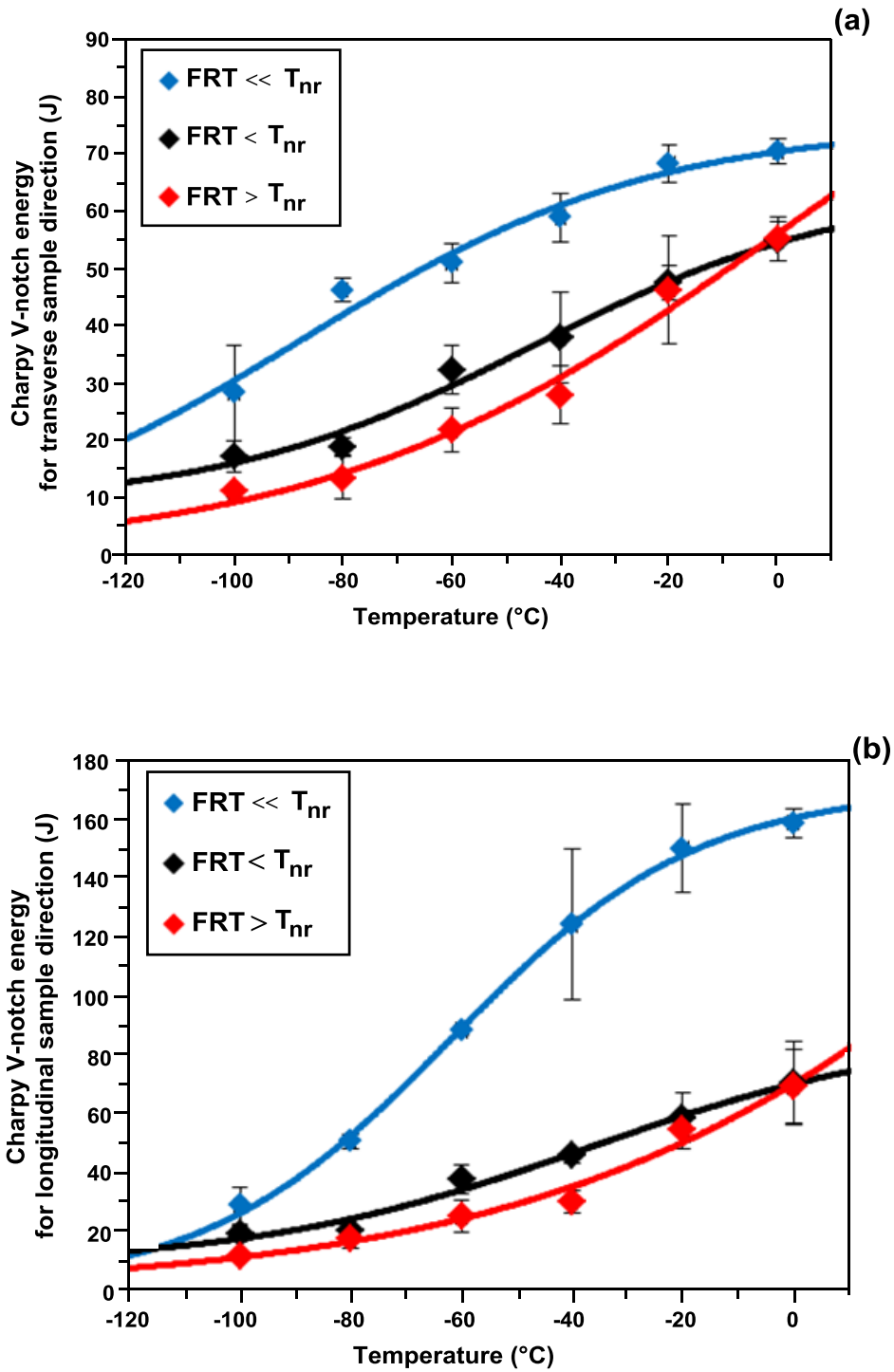


Figure 2. Charpy V-notch transition temperature curves for samples taken in the transverse (a) and in the longitudinal (b) directions of the three plates finish rolled at temperatures above and below  $T_{nr}$ . In the interest of clarity, each data point in the plot represents the mean value of six Charpy V-notch tests performed on three samples from the head and three from the tail position of each plate. The error bars represent one standard deviation.

In Figure 3, the single values of the Charpy V-notch energy measured at  $-40\text{ }^{\circ}\text{C}$  in the transverse direction are plotted as a function of the proof stress,  $R_{p0.2}$ . From this plot it can be deduced that the best combination of strength and toughness is obtained for the plate finish rolled at the lowest temperature. With a proof stress of more than 1100 MPa this plate demonstrates impact energies in the range of 50-70 J at  $-40\text{ }^{\circ}\text{C}$  for the transverse orientation. For the other two FRTs, lower proof stress and impact toughness values are observed. However, it is interesting to note that these plates show a very similar combination of strength and toughness despite different FRTs.

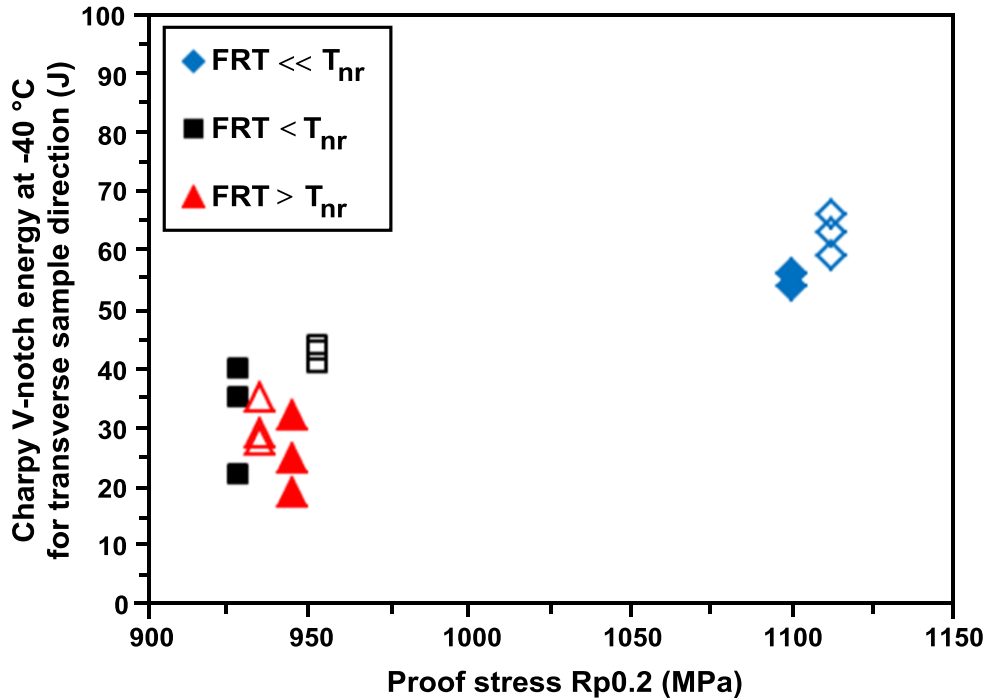


Figure 3. Single values of the Charpy V-notch impact energy measured at  $-40\text{ }^{\circ}\text{C}$  for the transverse direction as a function of the proof stress  $R_{p0.2}$ . Filled symbols represent the head position and open symbols the tail position of the plates.

To examine the effect of FRT on the hardenability of the plates, Vickers hardness profiles measured at the head and tail plate positions are plotted in Figure 4. For all three plates, the hardness is relatively constant across the through-thickness direction and in the region of 400 HV 10, as expected for a martensitic steel with a C content of approximately 0.15%. The plate finish rolled at the lowest temperature displays higher hardness values than the other two plates. Furthermore, it can be seen that the hardness profiles at the head and the tail positions are very similar. For example, for the plate with the intermediate FRT, the mean hardness at both ends differ by less than 6 HV 10.

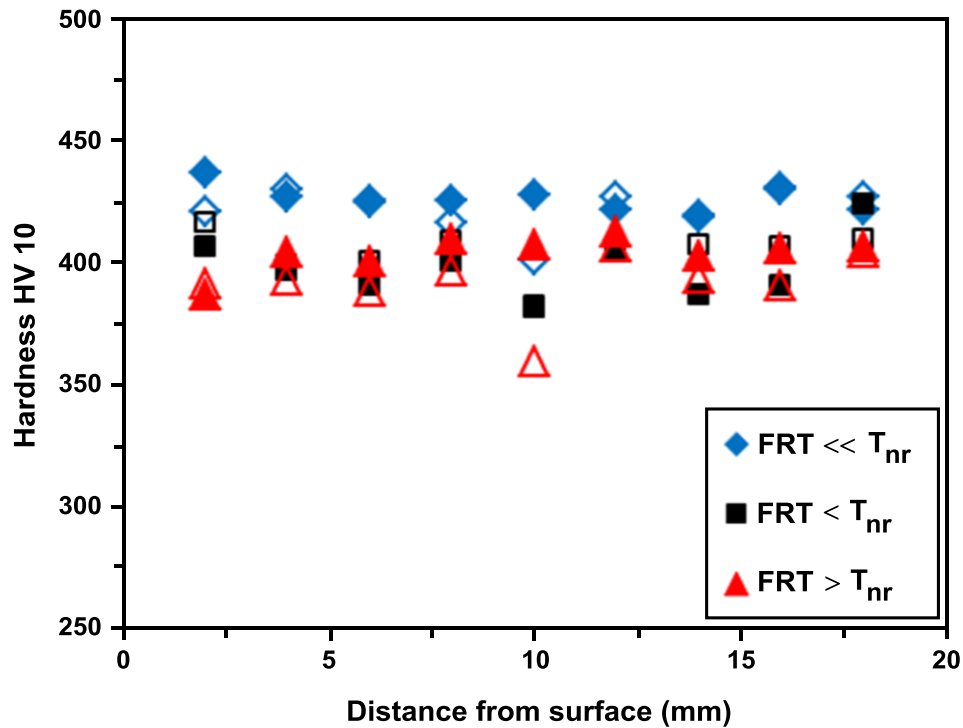


Figure 4. Vickers hardness profiles. Filled symbols represent the head position and open symbols the tail position of the plates.

Noticeable differences in the microstructure are observed depending on the FRT. This is highlighted in Figure 5, which shows optical micrographs of the surface, the quarter and the mid-thickness positions of the three plates. As the same microstructure was observed at both ends of the plates, only micrographs originating from the tail positions are presented. A relatively uniform microstructure, consisting of martensite and bainite, is visible for all plates throughout the plate thickness. Although not quantified, it seems that the bainite content increases slightly with decreasing FRT. A comparison of the micrographs further indicates that with decreasing FRT the microstructure becomes finer and elongated in the rolling direction for the lowest FRT.

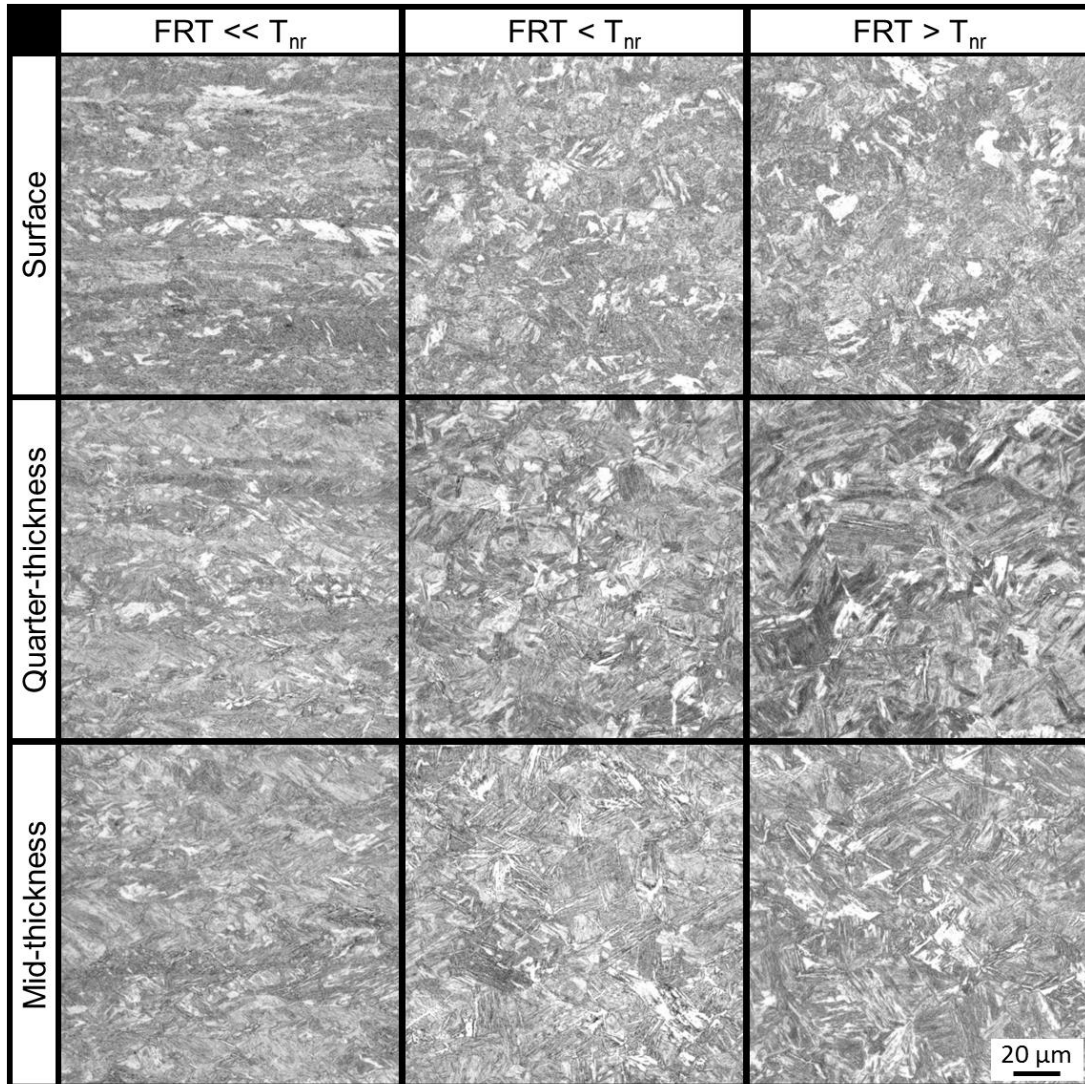


Figure 5. Light microscope images showing the microstructure at the surface, the quarter and the mid-thickness positions of the investigated plates.

To obtain additional insights into the microstructure prior to and post transformation, EBSD measurements were performed at the quarter-thickness positions of the plates and used to reconstruct the parent austenite structure. Consistent with the optical micrographs, the inverse pole figure (IPF) maps and the reconstructed austenite structure in Figure 6 reveal that with decreasing FRT the microstructure changes from coarse and fully recrystallized to fine and pancaked.

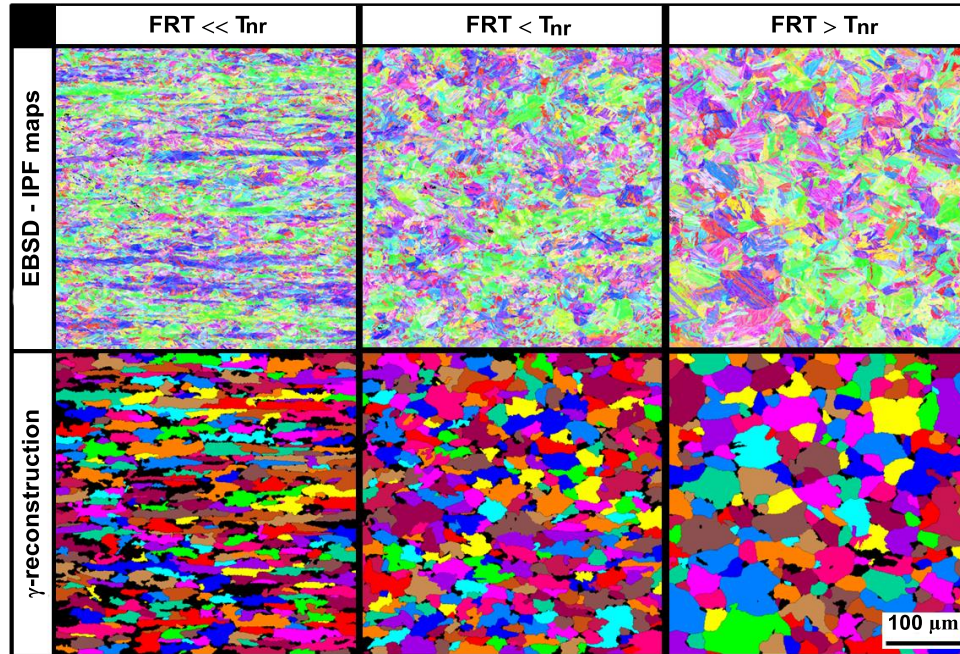


Figure 6. EBSD inverse pole figure (IPF) maps and austenite ( $\gamma$ ) reconstruction of the microstructure at quarter-thickness of the three plates finish rolled at different temperatures.

From the reconstructed austenite structure, the mean values of the equivalent diameter, as well as the Feret ratio, ie. the ratio between the minimum and the maximum Feret diameter or shortest and longest grain axis, were calculated and are listed in Table II. It can be seen that by decreasing the FRT in the tested range, the austenite grain size decreases from 25  $\mu\text{m}$  to 16  $\mu\text{m}$ . In addition, Feret ratios smaller than one indicate an elongation of the grains in the rolling direction for all three plates. While the stretching of the austenite grains with Feret ratios of 0.55-0.65 is relatively small for the plates finish rolled at temperatures close to  $T_{nr}$ , the Feret maximum (long axis) of the austenite grains in the plate finish rolled at the lowest temperature is, on average, 2.7 times larger than the Feret minimum (short axis).

Table II. Mean Values of Equivalent Diameter and Feret Ratio for the Three Plates Finish Rolled at Different FRT

	<b>FRT &lt;&lt; <math>T_{nr}</math></b>	<b>FRT &lt; <math>T_{nr}</math></b>	<b>FRT &gt; <math>T_{nr}</math></b>
Diameter ( $\mu\text{m}$ )	15.6	18.5	25.0
Feret ratio	0.37	0.55	0.64

The misorientation angle distributions from the EBSD measurements are shown in Figure 7. As expected for a martensitic/bainitic microstructure, the distributions display a pronounced peak at  $60^\circ$  and a smaller peak at around  $53^\circ$  for the three plates. Interestingly, the intensity of the peak at a misorientation angle of  $60^\circ$ , ie. the portion of high angle grain boundaries characteristic for martensite and lower bainite, decreases with decreasing FRT.

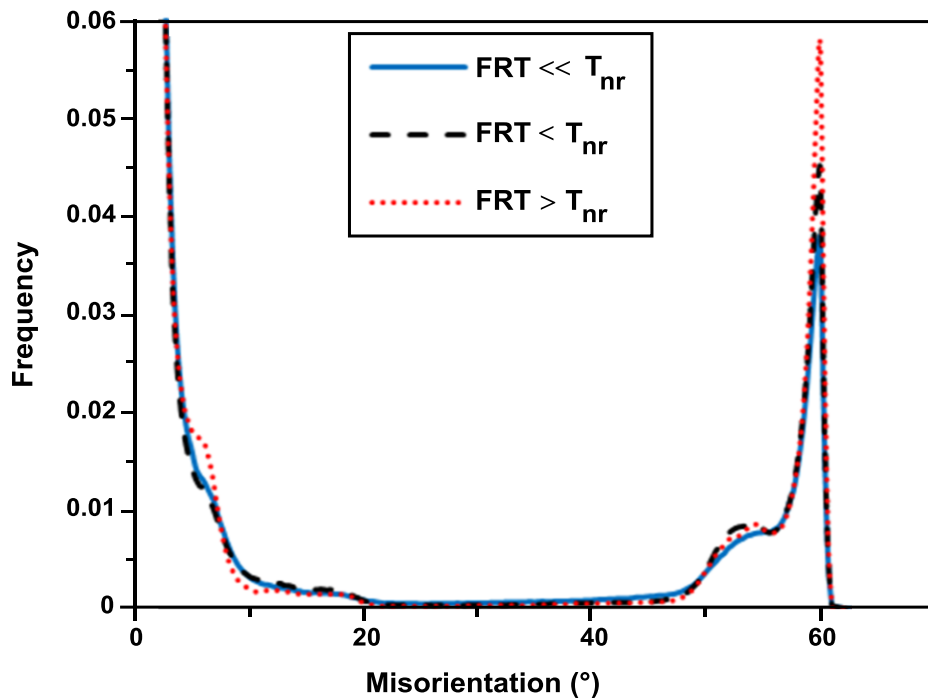


Figure 7. Grain boundary misorientation angle distribution of the investigated samples.

### Discussion

In the production line used for the current study, the cooling intensity for direct quenching is regulated by the water flow rate and the speed with which the plates are moved through the cooling device [12]. For plates with lengths of several tens of meters, the limited speed of motion might result in a certain time lag between the cooling of the head and the tail positions of the plates. Due to the longer time interval before quenching of the tail with respect to the head position, microstructural differences might arise between the ends of the plates. Depending on temperature and rolling history, recovery, recrystallization and grain growth might occur and affect the austenite structure before quenching. Furthermore, if the cooling start temperature at the tail of the plates drops below  $A_{r3}$ , ferrite transformation might be promoted, which is more critical at low FRTs.

For the tested plates, uniform properties and microstructures were observed at the head and the tail positions indicating that these effects can be neglected for the production parameters and alloy composition used. This is partly related to the fact that due to the high hardenability and relatively small plate thickness the tested plates needed a relatively short cooling time and thus were moved at a high speed through the cooling device. In addition, the Nb microalloying in the alloy used retards recrystallization and grain coarsening.

The highest hardness as well as the best balance between strength and toughness was observed for the plate finish rolled at the lowest temperature, ie. at a temperature significantly below  $T_{nr}$ . With an average hardness of approximately 425 HV throughout the thickness this plate exhibits an average impact toughness of approximately 60 J for the transverse and 125 J for the longitudinal sample direction at a test temperature of  $-40\text{ }^{\circ}\text{C}$ . These impact toughness values are much higher than those of the other two plates finish rolled at higher temperatures or conventional RQ plates of the same chemistry, which have a guaranteed V-notch toughness of 30 J at  $-40\text{ }^{\circ}\text{C}$  for the longitudinal sample direction.

Several factors account for the enhanced toughness of the plate finish rolled at the lowest temperature. First of all, transformation from work-hardened austenite effectively refines the resulting martensitic/bainitic microstructure, because, if hardenability is high enough, additional dislocations and deformation bands can assist the nucleation of these transformation products upon cooling [4]. As a consequence, the critical packet size for brittle fracture decreases leading to the improvement of toughness. Other effects that might contribute to the superior toughness are the shortening and the randomization of the martensite laths due to the ausforming effect as well as a specific crystallographic texture causing splitting behavior in the Charpy specimens [2,3,6].

It is interesting to note that despite the obviously finer martensite microstructure visible in the optical micrographs and the EBSD maps, the plate finish rolled at the lowest temperature shows a slightly smaller portion of high angle grain boundaries, characteristic for the martensitic structure, than the other two plates finish rolled at higher temperatures. Two factors may account for this effect: (1) Compared to the other two plates, a higher portion of random grain boundaries or misorientation angles, related to the parent austenite structure, is detected in the EBSD scan of the plate finish rolled at the lowest temperature, due to its finer austenite grain size. Consequently, the portion of high angle boundaries, characteristic for lower bainite and martensite, is reduced in this plate in comparison to the other two plates. (2) The hardenability of the steel might not be sufficient to completely suppress diffusion controlled transformations at the lowest FRT, where the deformation substructure promotes the nucleation of ferrite and granular bainite. Thus, the microstructure might contain other constituents besides lower bainite and martensite thus reducing the fraction of high angle grain boundaries in the plate finish rolled at the lowest temperature. In contrast, the less work-hardened austenite structure with a larger grain size in the plates finish rolled at higher temperatures favors the formation of martensite and lower bainite, explaining the higher peak at  $60^{\circ}$  in the corresponding misorientation angle distributions. However, to account for the high hardness/strength of the plate with the lowest FRT, it has to be assumed that the contribution from the softer microstructural constituents such as ferrite and granular bainite is small and overcompensated by the ausforming effect, ie. the strength/hardness increment related to the inheritance of the austenite dislocations in the transformed microstructure.

Although the average austenite grain size of the plate finish rolled at the intermediate temperature is only slightly larger than that of the plate finish rolled at the lowest temperature, it exhibits significantly lower impact toughness values. This shows that the reduction of the austenite grain size alone does not cause the improvement of toughness observed for the CR-DQ plate.

Furthermore, it is worthwhile noting that for the plate with the intermediate FRT the elongation of the austenite grains in the rolling direction is not too different from the plate finish rolled at a temperature above  $T_{nr}$ . Accordingly, it has to be assumed that the actual  $T_{nr}$  is lower than the theoretical  $T_{nr}$  calculated according to the equation by Boratto et al. [10], which is a reasonable assumption as this equation does not consider deformation due to rolling. Therefore, the microstructure of this plate might be more representative of a RCR process instead of a CR process. However, due to its fine grain size this plate still demonstrates comparable impact toughness values to the RQ counterparts. This is in contrast to most other studies on direct quenching, in which RQ plates generally show a higher impact toughness than RCR plates [3]. A possible explanation for this discrepancy is the Nb microalloying of the heat used for the current study, which drastically limits grain growth during hot processing.

### Conclusions

Using the example of wear resistant steels, this study has shown, from a practical point of view, the importance of Nb microalloying in direct quenching. Firstly it guarantees, even for long plates, a uniform microstructure along the full plate length when the process route is optimized. Further, by increasing the  $T_{nr}$  it enables hot rolling in a temperature interval between  $T_{nr}$  and  $Ar_3$ , which is crucial to obtain the desired microstructure and for the improvement of the mechanical properties related to low FRTs. Finally, during hot processing it limits the austenite grain growth leading to acceptable toughness levels even for higher FRTs.

### References

1. K.A. Taylor and S.S. Hansen, "Structure and Properties of Some Directly-Quenched Martensitic Steels," *Proceedings of the International Symposium on Accelerated Cooling of Rolled Steel*, ed. G.E. Ruddle and A.F. Crawley (Pergamon Press, 1987), 85-101.
2. K.A. Taylor and S.S. Hansen, "Effects of Vanadium and Processing Parameters on the Structure and Properties of a Direct-Quenched Low-Carbon Mo-B Steel," *Metallurgical Transactions A*, 22 (1991), 2359-2374.
3. R.K. Weiss and S.W. Thompson, "Strength Differences between Direct-Quenched and Reheated-and-Quenched Plate Steels," *Physical Metallurgy of Direct-Quenched Steels*, ed. S.W. Thompson, K.A. Taylor and F.B. Fletcher (TMS, 1993), 107-138.
4. K. Okamoto, A. Yoshie and H. Nakao, "Physical Metallurgy of Direct-Quenched Steel Plates and its Application for Commercial Processes and Products," *Physical Metallurgy of Direct-Quenched Steels*, ed. S.W. Thompson, K.A. Taylor and F.B. Fletcher, (TMS, 1993), 339-405.
5. N.C. Muckelroy, K.O. Findley and R.L. Bodnar, "Microstructure and Mechanical Properties of Direct Quenched Versus Conventional Reaustenitized and Quenched Plate," *Journal of Materials Engineering and Performance*, 22 (2013), 512-522.
6. B.L. Bramfitt and A.R. Marder, "A Study of the Delamination Behaviour of a Very Low-carbon Steel," *Metallurgical Transactions A*, 8 (1997), 1263-1273.

7. E. Kinnunen et al., "Development of a New Direct Quenched Abrasion Resistant Steel," *International Journal of Metallurgical Engineering*, 2 (2013), 27-34.
8. H. Song et al., "Impact Toughness of an NM400 Wear-Resistant Steel," *Journal of Iron and Steel Research, International*, 20 (8) (2013), 72-77.
9. H. Song et al., "Effect of Direct Quenching on Microstructure and Mechanical Properties of a Wear-resistant Steel," *Acta Metallurgica Sinica*, 26 (4) (2013), 390-398.
10. F. Boratto et al., "Effects of Chemical Composition on the Critical Temperatures of Microalloyed Steels," *Proceedings of the International Conference Physical Metallurgy of Thermomechanical Processing of Steels and Other Metals*, Tokyo, Japan, (Thermec-88, ISIJ International, 1988), 383-390.
11. C. Cayron, "ARPGE: A Computer Program to Automatically Reconstruct the Parent Grains from Electron Backscatter Diffraction Data," *Journal of Applied Crystallography*, 2007, no. 40:1183 – 1188.
12. A. Streisselberger et al., "Use of the MULPIC Cooling Equipment for the Production of High Strength Steel Plates," *Physical Metallurgy of Direct-Quenched Steels*, ed. S.W. Thompson, K.A. Taylor and F.B. Fletcher (TMS, 1993), 407-421.